Supporting Information

Innovative Approach for Preparing CNT-supported Pt-Nanoparticle Functional Electrocatalyst using Protic Ionic Liquids

Tomoya Sasaki, Reiko Izumi, Tetsuya Tsuda, and Susumu Kuwabata[*,†]

[†]Department of Applied Chemistry, Graduate School of Engineering, Osaka University
2-1 Yamada-oka, Suita, Osaka 565-0871, Japan

Corresponding Author
*kuwabata@chem.eng.osaka-u.ac.jp

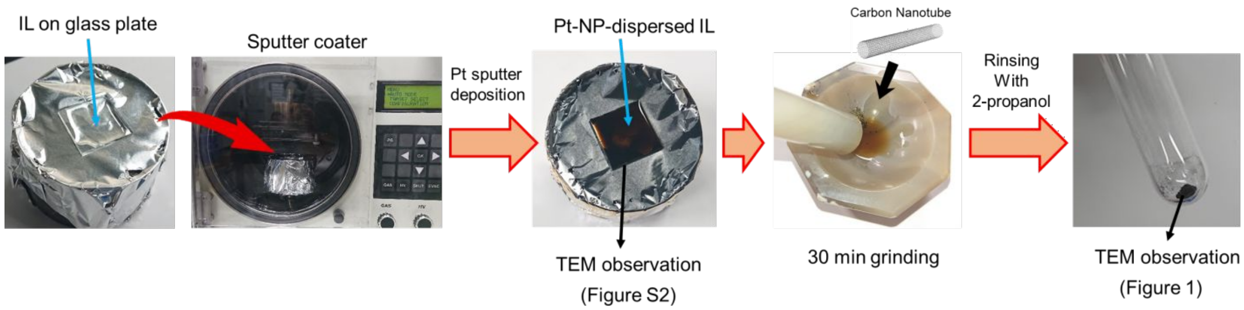

Figure S1. The procedure for the preparation of Pt-NP-modified CNT electrocatalysts.

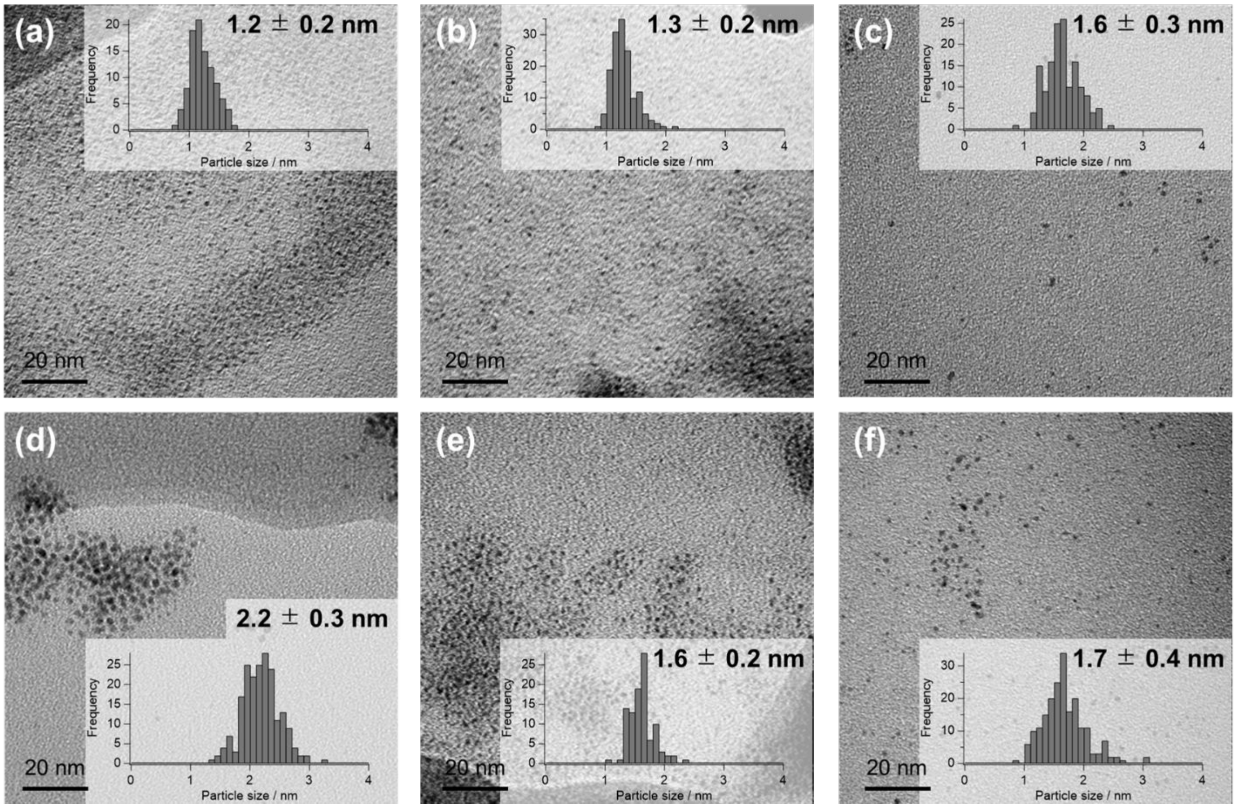

Figure S2. TEM images with particle size distribution of Pt NPs prepared by Pt-sputtering onto different ILs; (a) $[N_{1,1,1,3}]$[TFSA], (b) $[C_4mim]$[TFSA], (c) $[C_4mim]$[TfO], (d) [dema]HSO_4, (e) [dema][TFSA], and (f) [dema][TfO].

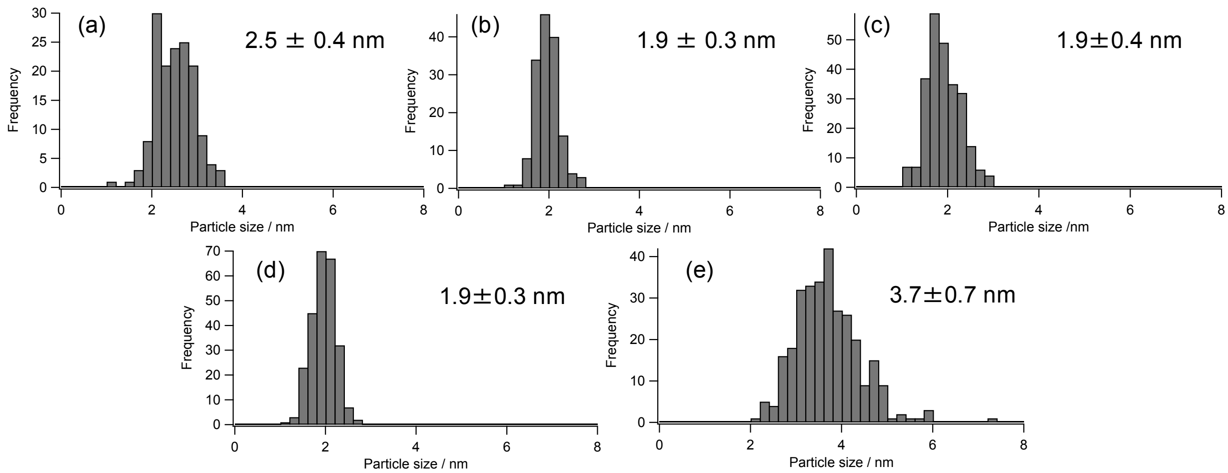

Figure S3. The particle size distributions of Pt-SWCNT prepared using (a) [dema]HSO_4, (b) [dema][TFSA], and (c) [dema][TfO], and those of (d) Pt-MWCNT and (e) commercial Pt–C.

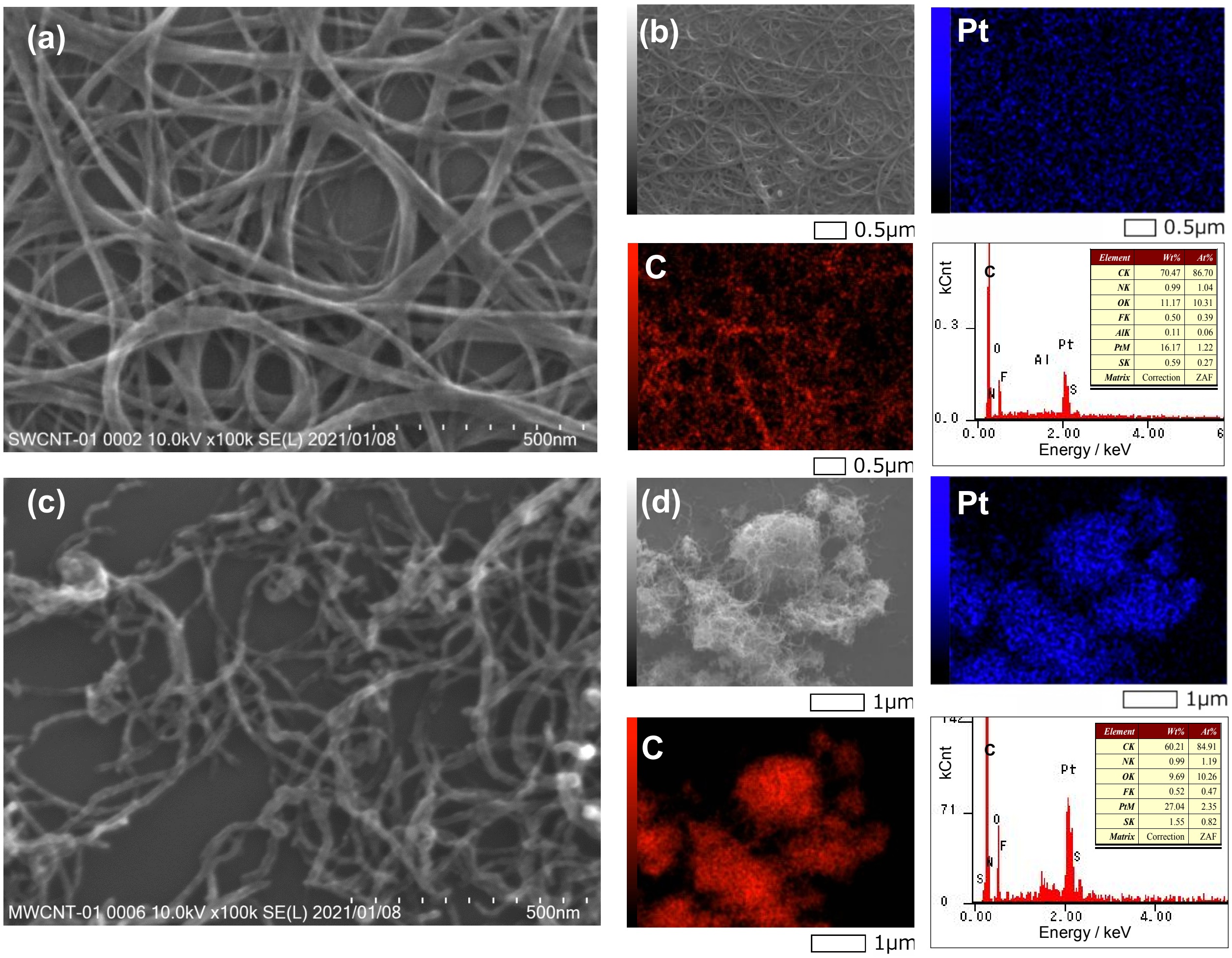

Figure S4. SEM images and SEM-EDX spectra and mapping images for Pt and C of (a,b) Pt-SWCNT and those of (c,d) Pt-MWCNT.

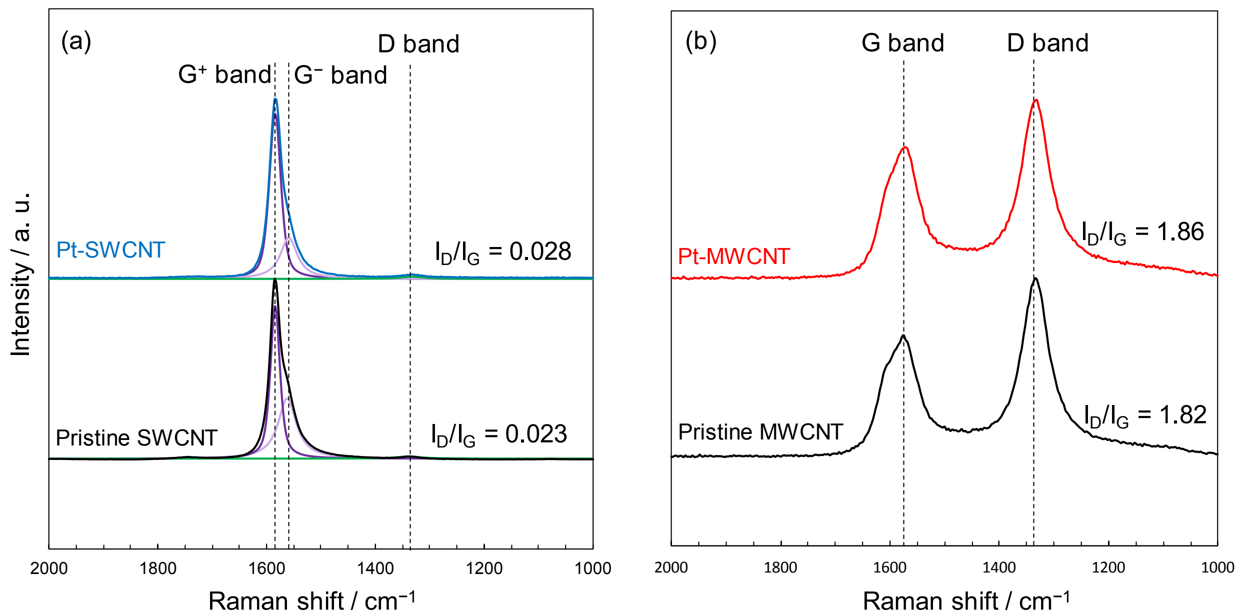

Figure S5. Raman spectra of (a) pristine SWCNT (black), Pt-SWCNT (blue), (b) pristine MWCNT (black), and Pt-MWCNT (red).

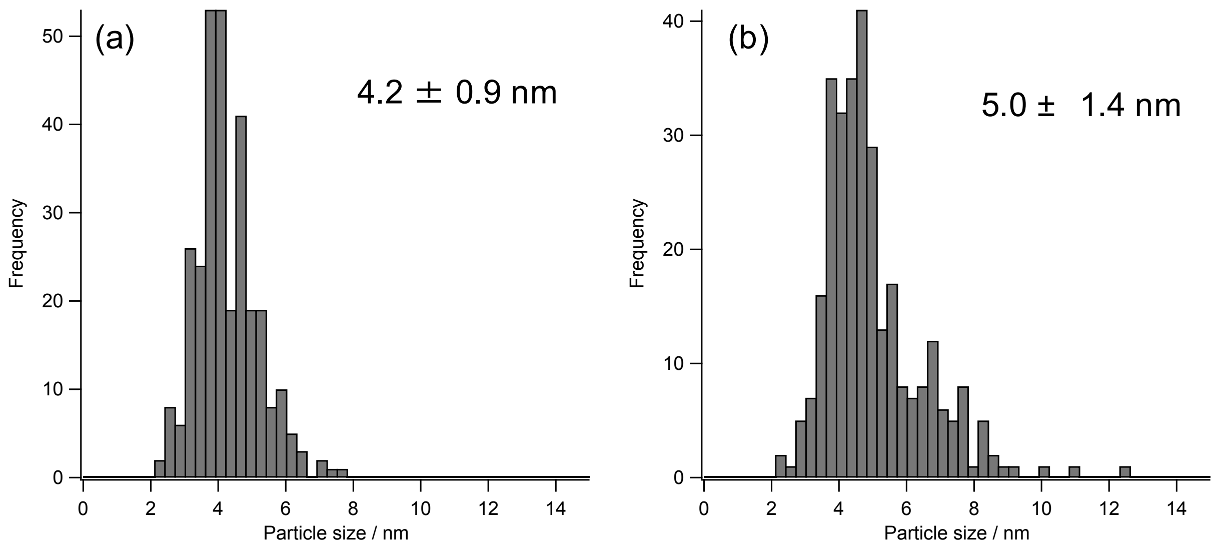

Figure S6. Pt NP size distribution of (a) Pt-MWCNT and (b) Pt–C subjected to 20,000-cycle ADT.

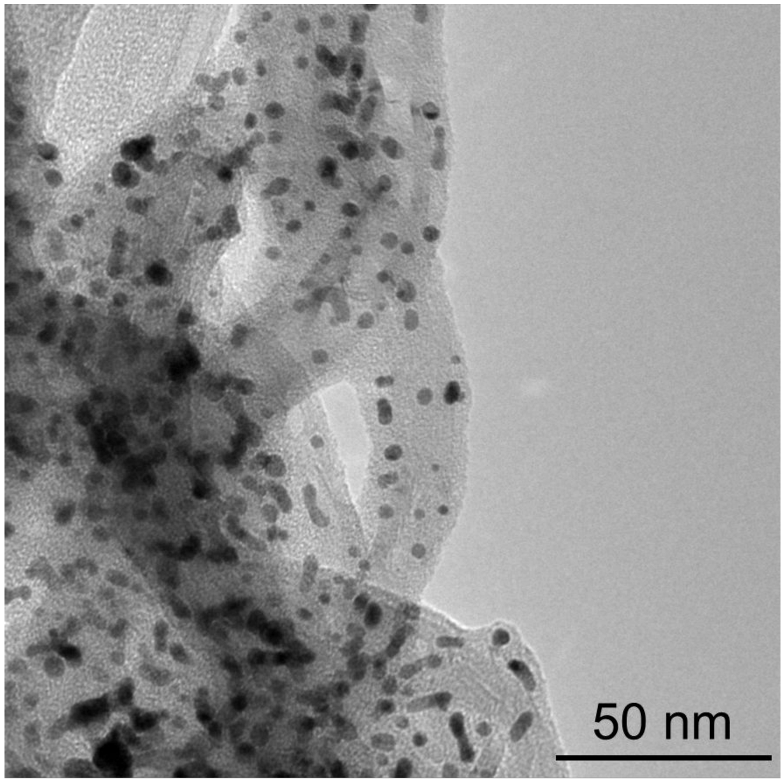

Figure S7. TEM image of Pt-MWCNT subjected to 20,000-cycle ADT.

Table S1. Performance comparison of CNT-supported Pt NP electrocatalysts reported in literatures

	CNT pretreatment	Immobilization of Pt NPs on CNT	ADT condition	ADT cycle number	Mean particle size /nm		ECSA /m^2 g_{Pt}^{-1}		Mass activity /A g_{Pt}^{-1}		Specific activity /A m_{Pt}^{-2}		TOF** /$atom_{Pt}^{-1}$ sec^{-1}		Reference
					Initial	After ADT	Initial	After ADT	Initial	After ADT	Initial	After ADT	Initial	After ADT	
Pt/MU-MWCNT	Unzipping CNT with potassium permanganate	Glycol reduction of Pt ion on CNT	Potential sweep, 0.6–1.1 V, 50 mV sec^{-1}	3000	1.95	-	103.4	82.2	174.5	93.3*	1.69	1.13	0.21	0.14	S1
Pt@CNx/CNT	Coating CNT with polyaniline and pyrolyzing it	Chemical reduction of Pt ion at same time as aniline polymerization on CNT	Potential sweep, 0–1.2 V, 50 mV sec^{-1}	1500	3.1 ± 0.9	3.2 ± 0.7	74.3	77.0	111 (0.85 V)	108.5 (0.85 V)	1.5 (0.85 V)	1.41 (0.85 V)	0.19 (0.85 V)	0.18 (0.85 V)	S2
PtNW/F-CNT	Sulfur-doping functionalized CNT by annealing with phenyl disulfide at 1000°C	Polyol reduction of Pt ion on sulfur-doped CNT with autoclave	Potential sweep, 0–1.5 V	3000	Nanowire	-	17.2	16.0	272 (0.9 V)	220 (0.9 V)	15.8 (0.9 V)	13.8 (0.9 V)	2.00 (0.9 V)	1.75 (0.9 V)	S3
Pt/Ppy-MWCNT	Coating CNT with polypyrrole	Copolymerization of Pt complex and pyrrole on CNT	Square potential wave, 0.6 V (3 sec)–1.0 V (3 sec)	30000	1.5 ± 0.5	-	96.0	63.8*	166 (0.9 V)	124 (0.9 V)	1.7 (0.9 V)	1.9 (0.9 V)*	0.22 (0.9 V)	0.24 (0.9 V)	S4
Pt/N-CNT	Coating CNT with Nafion	Polyol reduction of Pt ion on CNT	Potential sweep, 0.6–1.2 V, 100 mV sec^{-1}	6000	2.7	3.8	72.11	49.39	111 (0.9 V)	-	1.54 (0.9 V)	-	0.19 (0.9 V)	-	S5
Pt-Gd(5/1)-MWCNT	Coating CNT with polypyrrole	Copolymerization of Pt complex, pyrrole and Gd complex on CNT	Square potential wave, 0.6 V (3 sec)–1.0 V (3 sec)	30000	1.6 ± 0.9	-	68.8	36	350 (0.9 V)	120 (0.9 V)	5.0 (0.9 V)	3.4 (0.9 V)	0.63 (0.9 V)	0.43 (0.9 V)	S6
Pt-MWCNT	Nothing	Mixing Pt NP-dispersed IL and CNT at room temperature	Square potential wave, 0.6 V (3 sec)–1.0 V (3 sec)	20000	1.9 ± 0.3	4.2 ± 0.9	76.2	27.9	347.8 (0.9 V)	291.6 (0.9 V)	4.56 (0.9 V)	10.4 (0.9 V)	0.58 (0.9 V)	1.32 (0.9 V)	This work
Pt-SWCNT	Nothing	Mixing Pt NP-dispersed IL and CNT at room temperature	Square potential wave, 0.6 V (3 sec)–1.0 V (3 sec)	20000	1.9 ± 0.4	Nanorod (2.6 ± 0.8 /6.9 ± 3.6)	100.2	51.4	353.3 (0.9 V)	374.8 (0.9 V)	3.52 (0.9 V)	7.29 (0.9 V)	0.45 (0.9 V)	0.92 (0.9 V)	This work

*: calculated from a bar graph in the literature

**: TOF is given by

$$\mathrm{TOF}\ (\mathrm{atom}_{\mathrm{Pt}}^{-1}\mathrm{sec}^{-1}) = \frac{Specific\ activity\ (A\ m_{Pt}^{-2})}{4\ electron\ \times\ e\ (C\ electron^{-1})\ \times\ surface\ atom\ number\ (atoms_{Pt}\ m_{Pt}^{-2})}$$

where the average of the atomic density for Pt(111), Pt(110), and Pt(100) (1.50×10^{15}, 0.92×10^{15}, and 1.28×10^{15} [atom cm^{-2}], respectively) was used as the surface atom number.[S7]

References

(1) Shu, Q.; Xia, Z.; Wei, W.; Xu, X.; Sun, R.; Deng, R.; Yang, Q.; Zhao, H.; Wang, S.; Sun, G. Controllable Unzipping of Carbon Nanotubes as Advanced Pt Catalyst Supports for Oxygen Reduction, *ACS Applied Energy Materials* **2019,** 2, 5446-5455.

(2) Guo, L.; Jiang, W.-J.; Zhang, Y.; Hu, J.-S.; Wei, Z.-D.; Wan, L.-J. Embedding Pt Nanocrystals in N-Doped Porous Carbon/Carbon Nanotubes toward Highly Stable Electrocatalysts for the Oxygen Reduction Reaction, *ACS Catal.* **2015,** 5, 2903-2909.

(3) Hoque, M. A.; Hassan, F. M.; Jauhar, A. M.; Jiang, G.; Pritzker, M.; Choi, J.-Y.; Knights, S.; Ye, S.; Chen, Z. Web-Like 3d Architecture of Pt Nanowires and Sulfur-Doped Carbon Nanotube with Superior Electrocatalytic Performance, *ACS Sustainable Chemistry & Engineering* **2017,** 6, 93-98.

(4) Ichihashi, K.; Muratsugu, S.; Miyamoto, S.; Sakamoto, K.; Ishiguro, N.; Tada, M. Enhanced Oxygen Reduction Reaction Performance of Size-Controlled Pt Nanoparticles on Polypyrrole-Functionalized Carbon Nanotubes, *Dalton Trans* **2019,** 48, 7130-7137.

(5) Wang, Q.; Dai, N.; Zheng, J.; Zheng, J. P. Preparation and Catalytic Performance of Pt Supported on Nafion® Functionalized Carbon Nanotubes, *J. Electroanal. Chem.* **2019,** 854.

(6) Ichihashi, K.; Muratsugu, S.; Matsui, H.; Higashi, K.; Sekizawa, O.; Uruga, T.; Tada, M. Oxygen Reduction Reaction Performance Tuning on Pt Nanoparticle/Mwcnt Catalysts by Gd Species, *J. Phys. Chem. C* **2020,** 124, 26925-26936.

(7) Paulus, U. A.; Wokaun, A.; Scherer, G. G.; Schmidt, T. J.; Stamenkovic, V.; Markovic, N. M.; Ross, P. N. Oxygen Reduction on High Surface Area Pt-Based Alloy Catalysts in Comparison to Well Defined Smooth Bulk Alloy Electrodes, *Electrochim. Acta* **2002,** 47, 3787-3798.